

Wigner molecules in quantum dots

Boris Reusch,¹ Wolfgang Häusler,² and Hermann Grabert¹¹Fakultät für Physik, Albert-Ludwigs-Universität, D-79104 Freiburg, Germany²I. Institut für Theoretische Physik, Universität Hamburg, D-20355 Hamburg, Germany

(Received 30 August 2000; published 2 March 2001)

We perform unrestricted Hartree-Fock (HF) calculations for electrons in a parabolic quantum dot at zero magnetic field. The crossover from Fermi liquid to Wigner molecule behavior is studied for up to eight electrons and various spin components S_z . We compare the results with numerically exact path-integral Monte Carlo simulations and earlier HF studies. Even in the strongly correlated regime the symmetry-breaking HF solutions provide accurate estimates for the energies and describe the one-particle densities qualitatively. However, the HF approximation favors the formation of a Wigner molecule and produces azimuthal modulations of the density for even numbers of electrons in one spatial shell.

DOI: 10.1103/PhysRevB.63.113313

PACS number(s): 73.21.-b, 71.10.Ay, 71.10.Hf

The last decade has seen an enormous interest in quantum dots, i.e., a small number of two-dimensional (2D) electrons confined in a semiconductor heterostructure.¹ Experimentally, the N -electron states of these systems are studied by means of far-infrared,² capacitance,³ and transport spectroscopy,⁴ and exhibit features of quantization of charge and energy. Theoretically, a whole arsenal of methods for interacting electronic systems together with increasing computational power applies: exact diagonalization techniques,⁵ density functional theory,⁶ and quantum Monte Carlo methods.⁷ Recently, the very strongly correlated regime of small electronic densities has also attracted considerable interest.⁸⁻¹⁰ In particular, the formation of a Wigner molecule has been studied with quantum Monte Carlo (QMC),⁸ Hartree-Fock (HF),⁹ and configuration interaction¹⁰ calculations.

In this paper we reconsider the Hartree-Fock approximation, focusing on the crossover to the Wigner regime. An important practical and conceptual question to be clarified is how correlations beyond the mean field approximation contribute to the exact energy, and whether the Wigner molecule is described reliably within the HF approximation. In its unrestricted version, allowing for symmetry-broken solutions, the HF solution approaches the true ground state energy considerably better than with restricted HF which preserves the rotational symmetry of the Hamiltonian. This is achieved, however, at the expense of the quality of the wave functions.

In the case of a strong central potential in three dimensions, as in real atoms, the HF approximation is known to yield useful results for both energies and wave functions. Here, we show by comparison with exact Monte Carlo data⁸ that even for strong interaction *unrestricted* HF calculations can give very good estimates for the ground state energies of 2D quantum dots. Only tiny energy differences between different spin states cannot be resolved reliably. On the other hand, the charge density distribution resulting from unrestricted HF calculations cannot quantitatively describe the strongly correlated regime. For an even number of electrons per shell, the HF densities show effects of localization due to the strong electron interaction. Furthermore, within the HF approximation⁹ this crystallization sets in rather too early at higher densities than in the QMC study.⁸

We study a two-dimensional parabolic quantum dot with N electrons at zero magnetic field as discussed by many authors.⁵⁻¹⁰ Measuring energy in units of the oscillator energy $\hbar\omega_0$ and length in units of $l_0 = \sqrt{\hbar/m^*\omega_0}$, where m^* is the effective mass, the dimensionless Hamiltonian reads

$$H = \sum_{j=1}^N \left(-\frac{1}{2} \Delta_j + \frac{1}{2} r_j^2 \right) + \sum_{i<j=1}^N \frac{\lambda}{|\mathbf{r}_i - \mathbf{r}_j|} \\ \equiv \sum_{i=1}^N h_i + \sum_{i<j=1}^N w_{ij}. \quad (1)$$

Here we have introduced the dimensionless coupling constant $\lambda = l_0/a_B^* = e^2/\kappa l_0 \hbar\omega_0$ with the effective Bohr radius a_B^* and the dielectric constant κ . For example, $\lambda = 2$ corresponds to $\hbar\omega_0 \approx 3$ meV for a GaAs quantum dot. Since this Hamiltonian is rotationally invariant and spin independent, the exact eigenfunctions can be chosen as simultaneous eigenfunctions of the total angular momentum L_z^{tot} , the total spin S_z^{tot} and its z component S_z^{tot} . These eigenfunctions and corresponding densities are then rotationally invariant.

HF theory consists in approximating the many-particle wave function by an optimal single Slater determinant,

$$\Psi^{\text{HF}} = \frac{1}{\sqrt{N!}} \det[\varphi_i(\mathbf{r}_j)]_{1 \leq i, j \leq N}. \quad (2)$$

This HF Slater determinant is build up of single-particle orbitals $\varphi_i(\mathbf{r})$, which are expanded in the angular momentum basis of the 2D harmonic oscillator (Fock-Darwin states),

$$\langle \mathbf{r} | nM \rangle = \sqrt{\frac{n!}{\pi(n+|M|)!}} e^{iM\varphi_r} \mathcal{L}_n^{|M|}(r^2) e^{-r^2/2}. \quad (3)$$

Here, n and M are the radial and angular quantum numbers, and $\mathcal{L}_n^{|M|}$ is a Laguerre polynomial. In the unrestricted HF approximation an orbital has the expansion

$$\varphi_i(\mathbf{r}) = \sum_{\substack{n=0, \infty \\ M=-\infty, \infty}} u_{nM}^i \langle \mathbf{r} | nM \sigma_i \rangle, \quad (4)$$

where $\sigma_i = \pm \frac{1}{2}$ is the fixed electron spin of the i th orbital. This orbital is no longer an eigenfunction of the one-particle angular momentum; therefore the HF Slater determinant is in general not an eigenfunction of L_z^{tot} , but a deformed, symmetry-broken solution.¹¹ Similarly, the HF solution is in general not an eigenfunction of the total spin but only of its z component with eigenvalue $S_z^{\text{tot}} \equiv S_z = (N_\uparrow - N_\downarrow)/2 = \sum_i \sigma_i$.

Minimizing the HF energy $E^{\text{HF}} = \langle \Psi^{\text{HF}} | H | \Psi^{\text{HF}} \rangle$ and imposing orthonormality between the HF orbitals yields the HF equations for the expansion coefficients u_{nM}^i :

$$\sum_{\alpha} \left\{ \langle \gamma | h | \alpha \rangle + \sum_{\beta\beta'} (\gamma\beta | w | \alpha\beta') \rho_{\beta'\beta} \right\} u_{\alpha}^k = \epsilon_k u_{\gamma}^k. \quad (5)$$

Here, Greek indices abbreviate the quantum numbers of Eq. (3), for example, $\alpha \equiv (n, M, \sigma)$. The density matrix is defined by $\rho_{\alpha\alpha'} = \sum_{i=1}^N u_{\alpha}^i u_{\alpha'}^{i*}$, $\langle \gamma | h | \alpha \rangle$ is the one-particle matrix element, and

$(\alpha\alpha' | w | \beta\beta') = \langle \alpha\alpha' | w | \beta\beta' \rangle - \langle \alpha\alpha' | w | \beta'\beta \rangle$ denotes the antisymmetrized Coulomb matrix element, which we calculated analytically by transformation into relative and center of mass coordinates.¹³ The nonlinear self-consistent eigenvalue problem (5) for the expansion coefficients u_{α}^i is solved by iterative diagonalization starting from an initial guess for the density matrix. Several starting guesses have to be chosen in order to avoid local minima. The true minimum can also be identified by its one-particle density,

$$n^{\text{HF}}(\mathbf{r}) = \sum_{i=1}^N |\varphi_i(\mathbf{r})|^2, \quad (6)$$

which in the strong coupling limit mirrors the geometry of classical electrostatic point charges as we discuss below.

In our calculations we used up to 55 Fock-Darwin states for each spin direction. We present results for various sets of N, λ, S_z from $N=2$ to 8 particles covering the whole range of interaction strengths from $\lambda=2$ to 10.

The most important properties of the HF ground state energies can already be seen for $N=2$ (quantum dot helium). Here one knows the exact solution from diagonalization of the Hamiltonian for the relative motion.⁵ We have reproduced these results in Table I. The true ground state is always a singlet and the energy gap to the triplet vanishes slowly as $\lambda \rightarrow \infty$. In contrast, the HF approximation finds a triplet ground state for $\lambda \geq 5$, and the energies of singlet and triplet converge more rapidly.¹² The (absolute and relative) error is largest in the case of $S_z=0$ and $\lambda \approx 2$. In the polarized case the HF error increases monotonically with λ . These features of the HF energies can be seen for all N .

For $N > 2$ we compare with the path-integral QMC data of Ref. 8, which were obtained for the very low temperature $T = 0.1 \hbar \omega_0 / k_B$. The HF ground state energies are always above the QMC calculation energies for all particle numbers investigated so that the QMC data may serve effectively as zero temperature reference points. In the case of $N=5$ electrons, the QMC calculation gives a ground state spin of 1/2. In Fig. 1 we plot the energy difference of the different spin states with respect to the true ground state, $\Delta E = E_S - E_S^{\text{QMC}}$

TABLE I. Lowest energies of exact diagonalization and HF methods for $N=2$ and various S_z and coupling strengths λ . Relative error $(E_S^{\text{UHF}} - E_S^{\text{exact}})/E_S^{\text{exact}}$ in %.

λ	S_z	E^{exact}	E^{HF}	Relative error
2	1	4.142	4.168	0.7
2	0	3.721	4.034	8.3
4	1	5.119	5.189	1.4
4	0	4.848	5.182	6.8
6	1	5.990	6.096	1.8
6	0	5.784	6.107	5.7
8	1	6.787	6.919	1.9
8	0	6.618	6.930	4.7
10	1	7.528	7.679	2.0
10	0	7.384	7.686	4.2

$-E_{1/2}^{\text{QMC}}$, for various spin states as a function of the coupling strength λ . Again we see that ΔE is largest for $\lambda \approx 2$ and the smallest spin. It remains constant for $\lambda \geq 4$, resulting in a very low relative error of only 1–2% in the low density regime. The HF energy is very accurate in the case of $S_z = 5/2$, which becomes the HF ground state for $\lambda \geq 4$. This unphysically high ground state spin is due to the exchange term in the HF energy, which lowers the energy only for parallel spins. Therefore the spin ordering of the HF energies is just reversed.

For $N=8$ we give the HF energies in Table II. The QMC simulation predicts a transition of the ground state spin from $S=1$ to $S=2$ for $\lambda \geq 4$. Again, the HF method finds the wrong spin ordering in the correlated regime. The relative error is largest for the unpolarized states. The convergence of the HF energies for different S_z for $\lambda \geq 6$ can be understood in the classical picture of localized electrons without overlap and therefore no spin sensitivity.

Next we study the HF one-particle densities (6), where the crossover to the Wigner molecule is discernible. However,

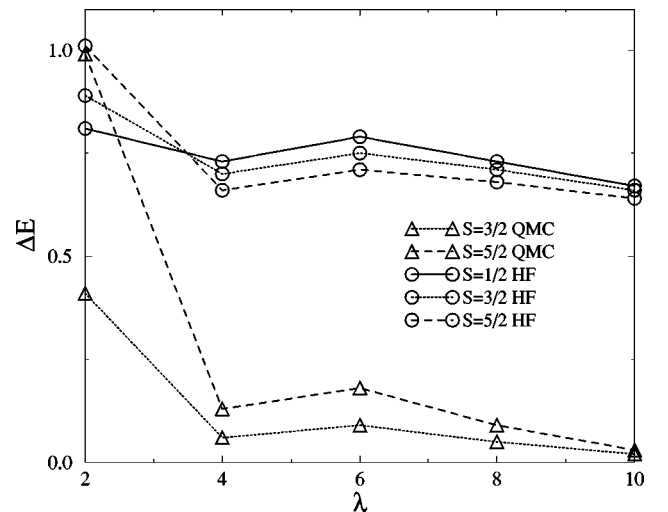


FIG. 1. $N=5$. Absolute energy differences from the QMC ground state ($S=1/2$), $\Delta E = E_S - E_S^{\text{QMC}}$, for various spins vs coupling constant λ .

TABLE II. Energies of QMC vs HF methods for $N=8$. Numbers in parentheses denote statistical errors of QMC. Relative error $(E_S^{\text{UHF}} - E_S^{\text{QMC}})/E_S^{\text{QMC}}$ in %.

λ	S_z	E^{QMC}	E^{HF}	Relative error
2	4	48.3(2)	48.534	0.5
2	3	47.4(3)	48.336	2.0
2	2	46.9(3)	48.243	2.9
2	1	46.5(2)	48.132	3.5
4	4	69.2(1)	69.735	0.8
4	3	68.5(2)	69.783	1.9
4	2	68.3(2)	69.826	2.2
6	4	86.92(6)	87.957	1.2
6	3	86.82(5)	87.999	1.4
6	2	86.74(4)	88.039	1.5
8	4	103.26(5)	104.492	1.2
8	3	103.19(4)	104.520	1.3
8	2	103.08(4)	104.547	1.4

one has to keep in mind that the deformation and structure of the HF densities arise from the symmetry-violating mean field and therefore may be artificial (whereas the HF energies are true upper bounds for the ground state energies). Second, we want to point out that a symmetry-breaking *Slater determinant* does not necessarily mean that its corresponding density displays a moleculelike structure. In Fig. 2 we display the densities for $N=2$ to 5 for strong coupling $\lambda=6$ and maximal spin $S_z=N/2$ (from $\lambda \geq 6$ the HF densities are essentially the same for all spins.). In the cases of two and four electrons they show quite distinct azimuthal maxima. This is not the case for the odd electron numbers 3 and 5: Surpris-

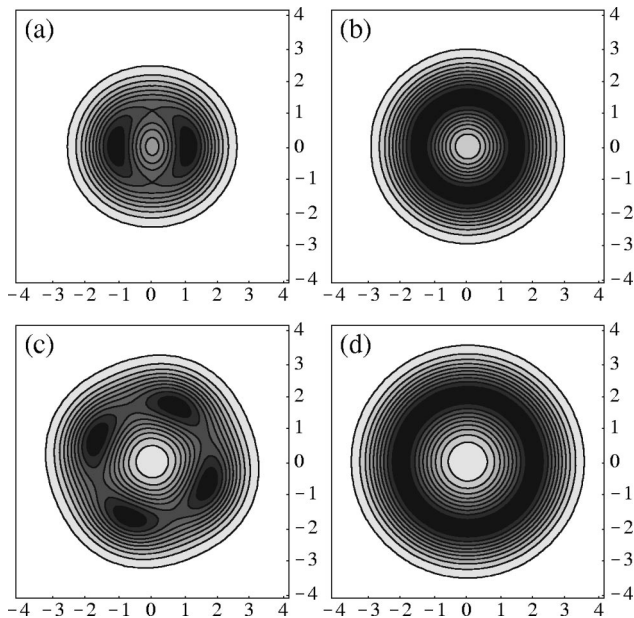


FIG. 2. Shaded contour plot of the HF density n^{HF} for $\lambda=6$, $S_z=N/2$, and different electron numbers. Contours lie at integral multiples of 0.1 times the maximal density. (a) $N=2$, (b) $N=3$, (c) $N=4$, (d) $N=5$.

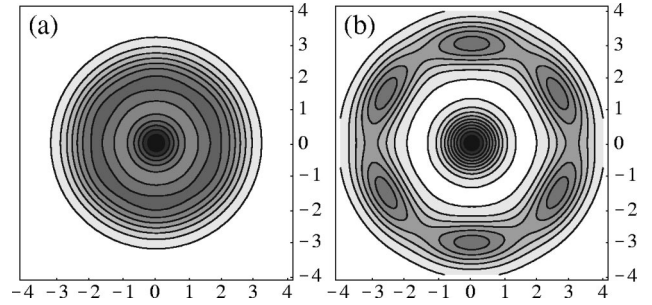


FIG. 3. Seven-electron Wigner molecule. HF density n^{HF} for (a) $\lambda=2$, $S_z=1/2$; (b) $\lambda=10$, $S_z=7/2$.

ingly, the HF densities, though belonging to a deformed Slater determinant, seem to be rotationally symmetric.

In order to understand this even-odd effect, consider an exact spin-polarized N -electron wave function Ψ_N for the Wigner molecule case. An even number of electrons in one spatial shell carries a *nonzero* angular momentum $\pm \hbar N/2$.¹⁴ In this fashion the HF wave functions with modulated density ($N=2,4$) can be interpreted as standing waves from a superposition of opposite angular momenta.¹⁵

However, the HF densities display the right classical filling for the spatial shells: From the maxima in the densities one can also read off the Brueckner parameter r_s , which is defined as the nearest-neighbor distance in units of a_B^* . These values r_s agree well with those obtained by QMC calculations and from a model of classical point charges. In Fig. 3 we show a seven-electron Wigner molecule for two interaction strengths. For $\lambda=2$ the HF density is already sixfold modulated with a central electron. Confronting this with the exact density in Fig. 1 of Ref. 8, we notice that the crystallization (as suggested by the HF densities) occurs too early. This explains why the authors of Ref. 9 observe

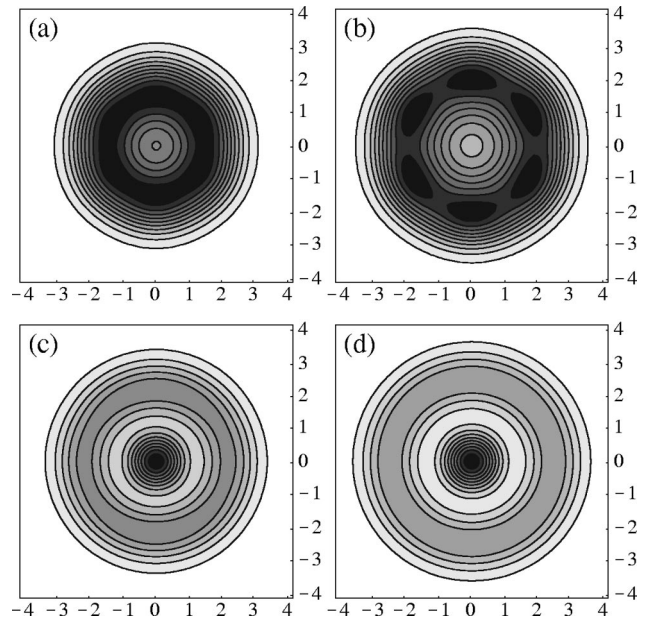


FIG. 4. $N=6$, $S_z=0$. Rearrangement from a six-fold [(a), $\lambda=2$] to a (deformed) fivefold geometry [(c), $\lambda=4$, $E=41.509$, (d), $\lambda=6$]. In (b), sixfold isomer at $\lambda=4$ with energy $E^*=41.838$.

Wigner crystallization for higher densities than in the exact QMC study.⁸ For higher λ the molecule with two spatial shells becomes more and more distinct. The maxima agree very well with the classical formula $r_s^3 = \lambda^4(2.25 + 1/\sqrt{3})$ for the sixfold geometry.

Finally, we show in Fig. 4 the crystallization for $N=6$ and $S_z=0$. This unpolarized case depicts a crossover from a sixfold arrangement [Fig. 4(a)] to a fivefold geometry [Figs. 4(c) and (d)]. The six-electron molecule was also studied by Reimann *et al.*,¹⁰ who found by means of configuration interaction calculations that the true ground state was unpolarized with a sixfold symmetry up to at least $\lambda \approx 3.5$. Within the HF approximation the $S_z=0$ state has already acquired a fivefold symmetry for $\lambda \geq 2.85$. In this range the HF density is distorted [$\lambda=4$ in Fig. 4(c)] and then again apparently circular for higher λ [$\lambda=6$ in Fig. 4(d)] with a central maximum. Figure 4(b) shows the sixfold isomer for $\lambda=4$, which is higher in energy by 0.33 than the ground state in Fig. 4(c). In contrast the spin-polarized state exhibits fivefold symmetry throughout the whole parameter range.¹⁶

In conclusion, we have shown in how far an unrestricted HF description of the Wigner molecule in quantum dots is reliable. The HF energies are good estimates of the true ground state energies especially for spin-polarized states. The energy differences for different spin states in the strongly interacting regime cannot be resolved properly. We find deformed HF densities in the regime of intermediate interaction up to $\lambda \leq 4$. For strong correlation the densities are azimuthally modulated for an even number of electrons in a shell and circular for an odd number per shell. The onset of this modulation is enhanced within the HF approximation, which leads to an overestimate of the value of the critical density for the crossover to the Wigner molecule. However, the HF densities mirror the classical filling scheme with the electrons arranged in spatial shells.

We thank R. Blümel, R. Egger, C. Stafford, and T. Vorrath for useful discussions. This research was supported by the SFB 276 of the Deutsche Forschungsgemeinschaft (Bonn).

¹L. Jacak, P. Hawrylak, and A. Wójs, *Quantum Dots* (Springer-Verlag, Heidelberg, 1998).

²B. Meurer, D. Heitmann, and K. Ploog, *Phys. Rev. Lett.* **68**, 1371 (1992).

³R. Ashoori, *Nature (London)* **379**, 413 (1996).

⁴L. P. Kouvenhouwen *et al.*, in *Mesoscopic Electron Transport*, Vol. 354 of *NATO Advanced Study Institute, Series E: Applied Sciences*, edited by L. L. Sohn, L. P. Kouvenhouwen, and G. Schön (Kluwer Academic Publishers, Dordrecht, 1997), pp. 105–214.

⁵U. Merkt, J. Huser, and M. Wagner, *Phys. Rev. B* **43**, 7320 (1991).

⁶K. Hirose and N. S. Wingreen, *Phys. Rev. B* **59**, 4604 (1999).

⁷J. Harting, O. Mülken, and P. Borrmann, *Phys. Rev. B* **62**, 10 207 (2000).

⁸R. Egger, W. Häusler, C. H. Mak, and H. Grabert, *Phys. Rev. Lett.* **82**, 3320 (1999); **83**, 462(E) (1999).

⁹C. Yannouleas and U. Landman, *Phys. Rev. Lett.* **82**, 5325

(1999).

¹⁰S. M. Reimann, M. Koskinen, and M. Maninen, *Phys. Rev. B* **62**, 8108 (2000).

¹¹We also performed *restricted* HF calculations where the angular momentum of φ_i is fixed.

¹²In the *restricted* HF the energies for different S_z do not merge, resulting in a considerably larger error for the unpolarized states.

¹³B. Reusch, Diploma thesis, University of Freiburg, 1998.

¹⁴A. J. Leggett, in *Granular Nanoelectronics*, Vol. 251 of *NATO Advanced Study Institute, Series B: Physics*, edited by D. K. Ferry, J. R. Barker, and C. Jacoboni, (Plenum, New York, 1991).

¹⁵A corresponding effect for weak interaction was observed in the density-functional study of Ref. 6.

¹⁶We were not able to reproduce the density of Fig. 2(c) in Ref. 9 unless we introduced a magnetic field [then we recovered the results of H.-M. Müller and S. E. Koonin, *Phys. Rev. B* **54**, 14 532 (1996)].